

Title:

Energy optimisation of plant factories and greenhouses for different climatic conditions

Author names and affiliations:

Till Weidner^a, Aidong Yang^a and Michael W. Hamm^b

^aUniversity of Oxford, Department of Engineering Sciences, Parks Road, Oxford OX1 3PJ, United Kingdom,

^bMichigan State University, Dept. of Community Sustainability, Natural Resources Building, 480 Wilson Road, Rm 312B, MSU, East Lansing, MI 48824, United States

till.weidner@eng.ox.ac.uk

aidong.yang@eng.ox.ac.uk

mhamm@msu.edu

Corresponding author:

Aidong Yang, University of Oxford, Department of Engineering Sciences, Parks Road, Oxford OX1 3PJ, United Kingdom, *aidong.yang@eng.ox.ac.uk*

Abstract

The trend to localise food production promises reduced reliance on increasingly uncertain global supply chains. Controlled-environment agriculture, in particular indoor vertical farming, is developing as part of this trend, to ensure a year-round supply of healthy food and protection from extreme weather events. However, high energy consumption is a major concern that could greatly impact the environmental sustainability of high-tech farms. Addressing the lack of comprehensive comparisons between different controlled-environment agriculture systems on a consistent basis, this work investigates the favourability of indoor vertical farms (i.e. plant factories) over modern ventilated open and closed greenhouses from an energy intensity perspective. This was based on a flexible yield-energy model incorporating detailed air conditioning system dynamics, which was developed to evaluate the influence of outside climate conditions on energy consumption and vegetable yield. The model was used to optimise the climate control strategy and to minimise hourly specific energy consumption for multiple systems, parameter settings, and locations. The hourly model performance is demonstrated for Stockholm, which indicates that advanced climate control allows for very low-energy operations in summer compared to winter. The results show a strong parametric sensitivity for the U-value of the cover, the target light intensity and the crop climate preference in all three systems, as well as the efficiency of lighting and water cooling for plant factories. Considering the yearly average for multiple locations, open greenhouses were substantially more energy-efficient than plant factories in all ten locations (from -45% in Reykjavík to -94% in Gauteng). The option to ventilate a greenhouse (open vs closed) had the greatest positive effect on specific energy consumption in less extreme climates (from -36% in Massachusetts to -83% in Gauteng) but increased water consumption considerably (from an average of ~2 l/kg to 26 l/kg). Although local availability of land and water plays a significant role in the choice between growing systems, the results imply that high-tech ventilated greenhouses perform significantly better than vertical farms from an energy perspective in most inhabited regions of the planet.

Keywords:

Controlled-environment-agriculture

Vegetable supply

Vertical farming

Climate control

Multivariate optimisation

Specific energy

1. Introduction

The consumption of both a good quantity and variety of fruits and vegetables is paramount for a healthy diet [1] and their steady supply is thus of critical importance to regional food systems. Increasing stress on supply chains from crises such as extreme weather events, geopolitical uncertainties and epidemics [2] leads to calls for more resilient food systems [3]. One way of achieving this is to focus on more regionalised food systems that simultaneously help achieve the UN Sustainable Development Goals [4]. This includes the scaling up of localised high-yield controlled-environment agriculture (CEA) systems, such as greenhouses (GH) and indoor vertical farms or plant factories (PF) [5]. Although these enable vegetable production in any climate or location, the space conditioning and additional lighting require high energy inputs [6]. The demand for energy, and in particular electricity, is projected to grow and it is often still sourced from fossil fuel due to the slow transition to renewable sources [7]. Therefore, a high carbon footprint penalty might be incurred for any potential gain in resilience [8] or self-sufficiency [15]. It is thus recommended to operate as energy-efficiently as possible [9], consider electrification opportunities [10] such as heat pumps [11], use renewable energy [12] and choose the CEA system that is more favourable in the local climate [13]. The favourability of specific CEA systems over others rests on multiple trade-offs, such as a closed CO₂-enriched environment versus an open ventilated system or the use of natural sunlight versus a more opaque structure with reduced heating and cooling needs, which is especially relevant in very hot or cold climates [14]. These complex trade-offs all affect the comparative energy intensity or specific energy use (i.e. kWh per kg produce), and policymakers and practitioners can benefit from knowing the expected energy use depending on local climate conditions and how it can be reduced through facility design and climate control.

A range of studies have been performed to address this complex challenge for the GH environment[16]. Most relevant for this work, Van Beveren et al. [17] created a dynamic model which optimises ventilation and heating control based on adjustable setpoints to achieve substantial energy savings of up to 75% during colder days. Cooling via fogging and ventilation was assessed by

Villarreal-Guerrero et al. [19], deriving combinational strategies to reduce energy consumption.

Vanthoor et al. [18] developed an economic model incorporating yield and energy use for operational and GH design heuristics, revealing that adapting to local climate conditions through seasonal whitewash, appropriate cover materials, thermal screens and variable cooling systems can reduce energy intensity. A comprehensive model including interactions between yield and energy demand was developed by Golzar et al. [20] and applied to different temperature, light and CO₂ setpoint scenarios, reporting specific energy benefits from optimised lighting and deviations from typical temperature setpoints in climate control. They also applied their model for different locations and found that heating and cooling requirements and thus CO₂ emissions varied greatly.

A simulation-based tool by Benis et al. [21] including vertical indoor farming revealed considerable climate-dependency of the CEA systems for tomato production; substantially lower energy consumption for the GH compared with vertical indoor farming in Lisbon but similar operational energy consumption in Paris, where it is colder [14]. A comprehensive comparison of CEA practices for lettuce in three different locations was carried out by Graamans et al. [14], based on PF specific models for evapotranspiration [22]. They confirmed the climate-dependency and revealed the potential benefits of PFs over GHs in cold (Sweden) and hot (United Arab Emirates, UAE) climates from an energy perspective. However, for GHs, they did not consider the impact of providing the same light and temperature conditions assumed for PFs through the year. A slightly different approach, by Li et al. [13], compared the resource intensity and profitability of open-field farming with CEA practices for several crops. They optimised the net present value based on operating parameters, including their effect on crop yield, and found that PFs with solar PV might be favourable for climate conditions in Singapore.

Previous efforts have highlighted certain aspects of comparing and improving CEA systems. However, it remains unclear how best-practice CEA systems would perform against each other in a given region. Simple heating and cooling needs derived from energy balances are usually considered, rather than the actual performance of electrified heating and dehumidification systems. Further, in

the comparative studies, more rigid climate setpoints instead of optimisation are employed [13,20,21,23], potentially favouring one system over the other. Thus, a comprehensive assessment is still missing which a) considers daily and annual fluctuations of outside climate conditions, b) incorporates energy-efficiency heuristics in facility design, c) models the air conditioning system and the spatial climate profile within a facility, d) optimises climate control and parameters affecting the yield of staple vegetables, while e) applying the same methodology for greenhouses and plant factories.

Addressing the above limitations of existing work, this study develops a new functional model which can optimise hourly space conditioning and specific energy consumption based on outside climate conditions for three types of CEA systems, namely plant factories and closed (non-ventilated) and open (ventilated) greenhouses. With the aid of the use of a reference vegetable basket, this has for the first time allowed these CEA systems to be compared, in their optimised performance, for a common set of diverse regions. The impact of the most relevant parameters and operational strategies has also been assessed to reveal how these factors may affect the comparative performance of these systems.

2. Methods

This work focuses on electricity consumption for lighting and climate control as they make up most of the energy consumed [6,14]. The specific energy consumption (i.e. energy consumption per unit output of produce), was optimised for three CEA systems, taking into account outside climate conditions at different locations. The energy consumption is equivalent to electricity consumption in this work. The optimisation models consist of mass and energy balances within the growing facilities and the air conditioning system and consider crop responses to internal climate conditions.

2.1 System overview

This sub-section explains the characteristics of the three systems, the mass and energy balances to simulate the interior conditions, technical aspects of the air conditioning system and the choice of crops.

2.1.1 Controlled-environment agriculture system design

The design of the CEA systems was derived from reported energy-efficiency measures with the aim of enabling a fair comparison between the systems based on the best technology available. Table 1 shows the main differences between the systems. The PF is an opaque, well-insulated and sealed structure. GHs are transparent structures that experience more pronounced heat exchange with the environment as well as some air infiltration and air exchange through ventilation (only for open ventilated greenhouses, OGH). Thus, GHs lose some of the irrigation and fogging water to the environment while PFs were considered to have a closed water circuit with continuous dehumidification. The PF benefits from multiple growing layers, increasing the ratio of growing to floor area [24]. The volume was chosen to be equal between the CAE systems to enable a fair comparison of space conditioning requirements. As current best practice to increase the productivity in GHs, sunlight is considered in this work to be supplemented with artificial light from light emitting diodes (LEDs) [25], to match the target daily light integral (DLI) of the plant. The standard efficacy of the LEDs was assumed to be 2.7 $\mu\text{mol/J}$ (equivalent to an efficiency of 59%). LEDs were the only source of light in PFs and, contrary to the GHs, the photoperiod was at night. A detailed description of the design and heuristics can be found in section 1 of the supplementary information (SI).

Table 1: The most relevant design parameters for the three CEA systems.

Category	Aspect	Plant factory (PF)	Closed greenhouse (CGH)	Open ventilated greenhouse (OGH)
Dimensions	Floor area (m ²)	1,250	2,500	2,500
	Productive space	60%	82%	82%
	Growing layers	4	1	1

Exterior	Growing area (m ²)	3,000	2,050	2,050
	Height (m)	8	4	4
	Volume	10,000	10,000	10,000
	Walls	Opaque structure	North-facing ¹ wall solid, other walls and roof translucent Ethylene tetrafluoroethylene (ETFE) or Polycarbonate (PC)	North-facing ¹ wall solid, other walls and roof translucent ETFE or (PC)
	Cover type	Insulated concrete	2 (ETFE), 2.27 (PC) or 0.5 (Reflective lens cover, RLC)	2 (ETFE), 2.27 (PC) or 0.5 (RLC)
	U-Value (W/(m ² *°C))	0.3	83% (ETFE), 70% (PC) or 28% (RLC)	83% (ETFE), 70% (PC) or 28% (RLC)
	Solar transmissivity	0		
	Infiltration rate (vol/h)	0	0.25	0.25
	Radiation at canopy vs. at light source	89% (reflective surfaces)	79%	79%
	LED cooling ratio	85% of waste heat	Flexible, up to 85% of waste heat	Flexible, up to 85% of waste heat
Space conditioning	CO ₂ level (ppm)	1600 ppm	1600 ppm	Variable supply (see SI 2.3)
	Water loss	None, fully recirculating	Loss only through infiltration	Loss through infiltration and venting
	Heating, ventilation and air conditioning (HVAC) system	Always dehumidification	Dehumidification or cooling only	Dehumidification or cooling only or none
	Other cooling options	-	Fogging	Venting and fogging
	Lighting	LED at night	Sunshine & LED during the day	Sunshine & LED during the day

1 ¹ For locations in the Southern hemisphere, this would be South facing.

2 2.1.2 Mass and energy balances

3 Simulating the interior of a CEA facility can be done in multiple ways, e.g. by using simplified

4 assumptions such as considering the space as well-mixed [26,27], or by a more complex calculation

of the spatial profile using computational fluid dynamics [28–30], which, however, makes optimisation very challenging. For this work, it is crucial to capture the interactions in the facility between the plants, the exterior climate and space conditioning efforts, which requires to model some degree of spatial heterogeneity [31,32]. Thus, a pragmatic approach was developed which differentiates three zones; inlet, centre, and outlet. The space was more well-mixed at lower venting (F_{vent}) and HVAC flowrates (F_{hvac}) and with a directional temperature and humidity gradient for higher venting and HVAC flowrates. The HVAC outlets were considered to be more distributed than venting inlets, hence venting elicited a more pronounced gradient than space conditioning through an HVAC. The main mass and energy flows used in the three systems are visualised in Figure 1. Heat exchange occurred between the outside and inside ($Q_{structure}$, Q_{solar} , $Q_{infiltration}$) of the facility and between the inside air and LEDs ($Q_{LED,PAR}$ and $Q_{LED,heat}$ influenced by $f_{LED,cooling}$), plants (Q_{SH}), cooling through fogging (Q_{fog}) and fans ($Q_{fans,hvac}$). Water was introduced into the air through infiltration ($m_{w,infiltration}$), plant evaporation ($m_{w,evap}$), fogging ($m_{w,fog}$) and ventilation (due to the difference in water vapour content), and was extracted as condensate ($m_{w,out}$). The air in the three different zones inside the facility and the HVAC inlet and outlet was described through the main properties including temperature (T_{suffix}), water vapour content (ω_{suffix}), relative humidity (RH_{suffix}) and enthalpy (h_{suffix}) where “suffix” refers to the specific locations in the system.

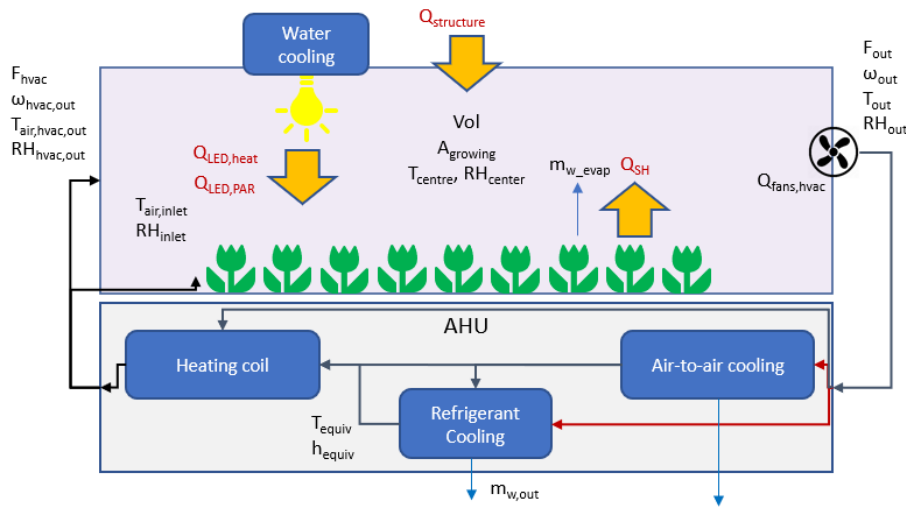
The HVAC operated either in dehumidification mode (including a reheating step), in cooling-only mode or in heating-only mode (only applicable to GHs). The conditions at the inlet and outlet of the HVAC were used to determine the air conditioning requirements. The centre conditions of the CEA facility were used to determine evapotranspiration and the effect of infiltration. Lower and upper climate parameter bounds were applicable at all three locations. In the OGH, the flow into the GH was made up of outside and conditioned air. The total electricity consumption (Equation 1) was determined by adding the electricity consumption of the air-to-air cooling, ($E_{fans,a2a}$), refrigeration cycle (E_{RC}), the air-source heat pump (E_{ASHP}), the LED ($Power_{LED}$) and the LED cooling ($E_{cool,LED}$), the fans inside the growing facility ($E_{fans,hvac}$), the fogging system (E_{fog} , GH only), and the

1 ventilation fans ($E_{fans,vent}$, OGH). The loss of water and CO_2 due to infiltration and venting was also
 2 considered (SI 2.2 and 2.3).

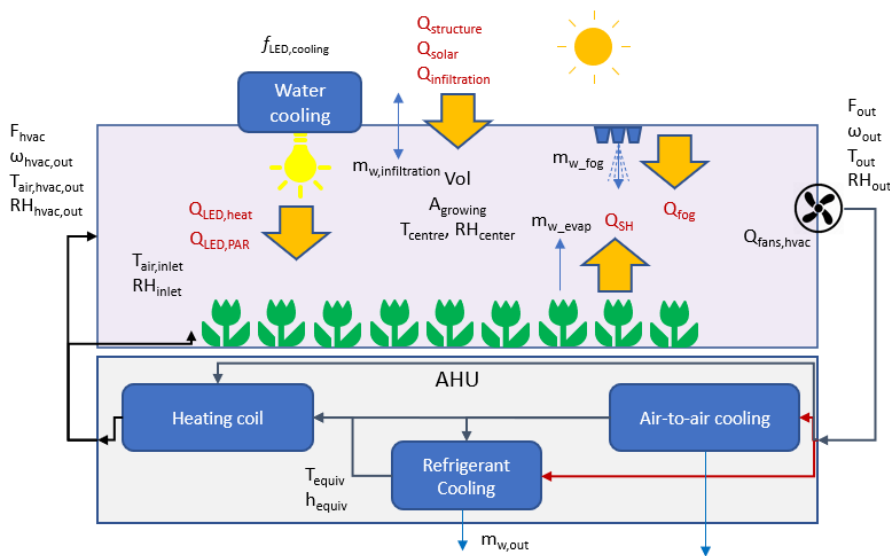
$$E_{total} = E_{RC} + E_{fans,a2a} + E_{ASHP} + Power_{LED} + E_{cool,LED} + E_{fans,hvac} + [E_{fog} + E_{fans,vent}] \quad Eq. 1$$

3
 4 All equations used can be found in the SI; the primary mass and energy balances in SI 2.1, exchanges
 5 with the environment in SI 2.2, CO_2 level in the OGH in SI 2.3, thermodynamic relations in SI 2.4 and
 6 physical relations in SI 2.5.

Plant factory (PF)



Closed greenhouse (CGH)



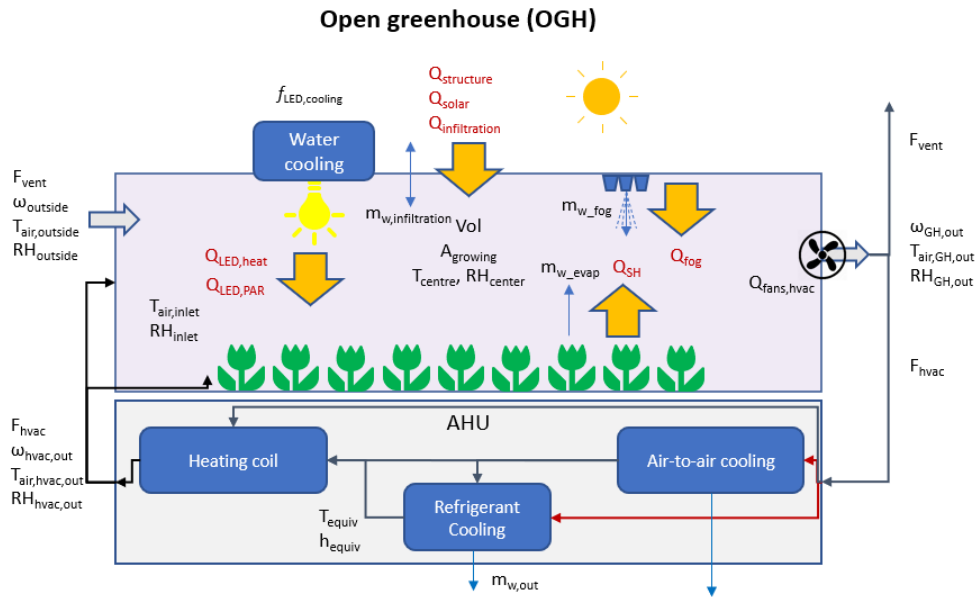


Figure 1: Schematic of the mass and energy balances of the three CEA systems. The large arrows depict energy fluxes and the small arrows material flows.

2.1.3 Air conditioning system

Besides heating and cooling requirements, indoor growing facilities need to remove moisture generated by the plants. To adequately assess and optimise the energy use of CEA facilities, the behaviour of the HVAC system has to be explicitly modelled [33] and this work does so by incorporating variable interior and exterior climate conditions. Although currently most GHs are heated with fossil-fuels [34], this work considers air-source heat pumps (ASHP) for the heating requirements. First, significant carbon abatement potential exists by electrifying the equipment [11,34,35], in particular with electricity from renewable sources. ASHPs were chosen over slightly more efficient ground-source heat pumps due to significantly lower upfront costs and lower dependency on shallow aquifers [36]. A schematic of the HVAC is shown in Figure 2, which together with the ducts and fans makes up the HVAC system.

The diagram illustrates a two-stage refrigeration system for a data center. It is divided into three main sections by vertical dotted lines:

- Left Section (Process Side):**
 - Process side heat pump HEX:** A vertical rectangular heat exchanger.
 - Process side refrigeration cycle HEX:** A vertical rectangular heat exchanger.
 - Air cooled evaporator of heat pump:** A horizontal rectangular unit with a fan icon, connected to the top of the process side heat pump HEX by a red line.
 - Air cooled condenser of refrigeration cycle:** A horizontal rectangular unit with a fan icon, connected to the top of the process side refrigeration cycle HEX by a blue line.
 - Process side heat pump:** A circular unit with a fan icon, connected to the bottom of the process side heat pump HEX by a red line.
 - Process side refrigeration cycle:** A circular unit with a fan icon, connected to the bottom of the process side refrigeration cycle HEX by a blue line.
 - Flow:** Red lines indicate the flow of the heat pump cycle, and blue lines indicate the flow of the refrigeration cycle.
- Middle Section (Inter-stage):**
 - Process side refrigeration cycle HEX:** A vertical rectangular heat exchanger.
 - Process side heat pump:** A circular unit with a fan icon, connected to the bottom of the process side refrigeration cycle HEX by a red line.
 - Process side refrigeration cycle:** A circular unit with a fan icon, connected to the bottom of the process side refrigeration cycle HEX by a blue line.
 - Flow:** Red lines indicate the flow of the heat pump cycle, and blue lines indicate the flow of the refrigeration cycle.
- Right Section (Facility Side):**
 - Air-to-air plate heat exchanger:** A rectangular unit with a diagonal line, connected to the top of the process side heat pump HEX by a red line.
 - From facility (hvac,in):** A horizontal line entering the top of the air-to-air plate heat exchanger.
 - Process side heat pump:** A circular unit with a fan icon, connected to the bottom of the air-to-air plate heat exchanger by a red line.
 - Process side refrigeration cycle:** A circular unit with a fan icon, connected to the bottom of the air-to-air plate heat exchanger by a blue line.
 - Flow:** Red lines indicate the flow of the heat pump cycle, and blue lines indicate the flow of the refrigeration cycle.

The HVAC features a typical refrigeration cycle (RC) in which the heat gained by the refrigerant in the cooling process may either be rejected back to the stream (for reheating after dehumidification) or, for cooling-only processes, to an air-cooled condenser. The concept of the (upstream) air-to-air heat exchanger was inspired by Graamans et al. [33] and expanded with the option for partial bypassing to reduce the use of this heat exchanger (HEX) at warmer ambient conditions (where this HEX would become inefficient due to a lower heat exchange temperature difference). This was mathematically realised by combining the NTU method [37] and a cooling ratio term to iteratively calculate the heat exchange area used for cooling-only and the cooling plus condensation section of the HEX. The relevant state variables of the RC were related to operating conditions via polynomials to allow for a flexible optimisation of these conditions, including particularly a detailed calculation of the coefficient of performance (COP), which also depends on the outside climate. The COP of the LED water cooling was approximated using the same concept. Considered for the electricity consumption were the two compressors, the outside and inside air fans of the RC and ASHP and the two fans of

the air-to-air HEX (inside and outside air flows). Further details about the concepts, functionality and dimensions are listed in SI 3.1 and all equations are listed in SI 3.2.

2.1.4 Vegetable selection

Crops differ in their characteristics; hence optimum settings of the climate system are crop dependent. Since this study intends to assess the production of staple vegetables in GHs and PFs, a vegetable basket, i.e. a proxy, has been defined reflecting the properties of the six most consumed vegetables (www.fao.org/faostat/en/) that can be produced in soilless growing systems (tomato, bell pepper, lettuce, broccoli, spinach, summer squash). A vegetable basket proxy ensures that a global comparison of electricity use is not favouring a particular cultivar (e.g. high yield vs. low yield [24]) or climate (e.g. hardy vs tender vegetables) while also approximating the actual demand that would need to be satisfied. The vegetable basket is composed of lettuce, broccoli, bell pepper, spinach, zucchini (12.5% each) and tomato (40%). The vegetable basket requires a DLI of 13.7 mol/day with a photoperiod of 14 hours (in the PF), resulting in a reference yield of 38 kg/m²/year. The properties of the crops making up the basket are detailed in SI 4.4.

2.2 Plant growth and climate settings

This sub-section explains how evapotranspiration, productivity, the interior climate boundaries and exterior climate conditions were determined.

2.2.1 Evapotranspiration

To calculate the amount of water transpired by the plants (i.e. evapotranspiration), this work uses the method employed by Graamans et al. [22], which balances the latent and sensible heat with the radiation received by the plant. Equation 2 [22] computes the latent heat equation, depending on the vapour concentration difference (VCD), the leaf area index (*LAI*), the heat of vaporization at the leaf surface (λ_{leaf}), and the aerodynamic (r_a) and canopy resistance (r_c).

$$LH = LAI * \lambda_{leaf} * \frac{VCD}{r_c + r_a} \quad Eq. 2$$

The canopy resistance is derived from the stomatal resistance and is calculated differently to Graamans et al. [22] as includes a radiation term, a vapour pressure deficit (VPD) term and a CO₂ term [38–40]. A detailed explanation and rationale for the method and values chosen, including the equations employed, is described in SI 4.1 and a description of all terms is provided in the nomenclature.

2.2.2 Yield and specific energy consumption

The optimisation aims to determine the minimum energy requirements per kg crops produced. This specific energy as electricity (kWh/kg crop) requires an approximation of the daily or hourly crop growth, influenced by temperature, PAR received and CO₂ levels of the inside air. Crop or yield modelling has been carried out by many studies [41,42] and applied explicitly to indoor farms in similar assessments combining energy consumption and crop yield [12,20]. In general, the yield models differ in their estimated yield and accuracy due to a limited understanding of the physical and biological processes for each crop [42]. Adapted models were therefore selected for this work that were both (1) straightforward to apply and (2) featured parametric sensitivities that reflect results from experimental studies and reports from growers. Although structural (e.g. cells) plant growth also occurs at night, the main driver for it is the existence of photosynthesis products generated during the photoperiod [43]. In this work it is thus assumed that reference yields in kg m⁻² year⁻¹ for year-round production ($Y_{ref,annual}$) with artificial light supplementation can be converted to daily growth values which are distributed over the photoperiod (t_{photo} , see SI 4.3) as shown in Equation 3 to obtain hourly growth or yield (Y_{hourly}). Deviations from the reference conditions are reflected in a change of the yield factor (YF_{total}) which is determined for each of the spatial zones within a CAE by relations between yield and PAR, yield and temperature, and yield CO₂ levels (see SI 4.2). The specific hourly energy (SE_{hourly} , Equation 4) to be optimised for the photo or day period was then assessed by using this hourly yield (SI 4.3), the growing area ($A_{growing}$) and the total electricity

consumption (from Equation 1). Finally, the average specific energy for the given day ($SE_{product}$, Equation 5) was assessed by aggregating the hourly yield during the photoperiod (from t_1 to t_2) and dividing it by the total energy use during the day.

$$Y_{hourly}(t) = \frac{Y_{ref,annual}}{365 \frac{days}{year} * t_{photo}} * YF_{total}(t) \quad Eq. 3$$

$$SE_{hourly}(t) = \frac{E_{total}(t)}{Y_{hourly}(t) * A_{growing}} \quad Eq. 4$$

$$SE_{product} = \frac{\sum_{t_1}^{t_2} E_{total}(t)}{\sum_{t_1}^{t_2} Y_{hourly}(t)} \quad Eq. 5$$

2.2.3 Interior climate

For the day or the photoperiod, the minimum and maximum permissible temperatures at the inlet and the outlet of a GH or PF was such that the hourly yield is at least 85% of its optimum value. This was done to ensure that the specific energy consumption is not maximised by sacrificing yield through shutting off the climate system since this would be contradictory to the business model of high-tech farming operations. For the night or dark period, the permissible temperature range which was assumed to not negatively affect the yield was obtained by reducing the optimum day temperature by 8 °C [21] and allowing a temperature of +/- 4 °C around the optimum night temperature [44]. To capture the different preferred temperature ranges of certain cultivars and crops in the vegetable basket, the sensitivity to the temperature ranges (shown in Table 2) has been assessed in the scenario analysis.

Table 2: Permissible day- and night-time temperature ranges and optimum temperature used in the optimisation model for three different crop climate preferences.

Preferred climate	T _{opt} (C)	T _{min} , T _{max} (photo, °C)	T _{min} , T _{max} (night, °C)
Mild (basket)	22.1	15.6, 28.0	10.1, 18.1
Warm	27	20.6, 32.5	15, 23
Cold	16	10.5, 21.2	4, 12

Evapotranspiration is directly dependent on the VPD, rather than through the water pressure or the relative humidity. It is thus a more relevant factor for determining a range of climate conditions

conducive to optimum plant growth [45]. Several studies have reported different VPD ranges that have not negatively affected crop growth in their experiments, sometimes with an optimum range and an acceptable range [46,47]. For this work, a permissible range of 4 hPa to 12 hPa was chosen to constrain VPD inside the CEA facility for all locations.

2.2.4 Exterior climate

Hourly optimisation of the climate control system requires knowledge about outside temperature, vapour pressure and incoming solar radiation (global horizontal irradiation, GHI) for every hour of the day. Since the optimisation was carried out for each hour within a typical day for a given month, available data on the average minimum and maximum daily temperatures within a particular month were used to construct temperature curves while average daily solar radiation and sun-hours were used to construct the solar radiation profile. For the sun-hours, second-order polynomials were developed which relate the latitude to the average daily hours of sunshine set according to the 15th day of the respective month (see SI 5.1). The GHI values used (daily average) already accounted for the effect of cloud cover. The vapour pressure was assumed to be constant throughout the respective day but never exceeding the saturation level. The data was obtained from <https://www.worldclim.org/> and is described in Fick and Hijmans [48]; the methodology to construct temperature and solar radiation curves is described in Weidner and Yang [15] the solar noon was set to 12:30 PM. Eighteen metropolitan regions were selected for this analysis, covering most of the habitable climate zones on Earth. They were chosen to ensure a sufficiently different combination of latitude (seasonality), temperature, humidity and solar radiation. Further information on geoprocessing steps can be found in SI 5.2, and a table with information on climate parameters can be found in SI 5.3.

2.3 Optimisation

The optimisation of the specific energy was carried out for each CEA system on an hourly basis in order to obtain sufficiently accurate prediction [17]. This results in a 24-hour operational profile

which describes the performance of the CEA system for the given location on a typical day within the given month. This calculation was then repeated for every month in multiple locations to obtain the average annual specific energy consumption. The inside air flowrate through the HVAC (F_{hvac}) and the share of it send through the air-to-air HEX ($f_{a2a,share}$), together with the temperature ($T_{hvac,out}$) and relative humidity ($RH_{hvac,out}$) of the HVAC outlets and the external air speed through the air-to-air HEX ($u_{air,a2a,ext}$) were adjusted by the optimisation to achieve minimum specific energy consumption. Further variable elements of control were the fogging flowrate ($m_{w,fog}$) in both GHs and the venting flowrate (F_{vent}) in the OGH. The system was constrained by a minimum air exchange rate (AER_{min}), a suitable VPD and temperature range at the inlet (VPD_{in}, T_{in}) and outlet (VPD_{out}, T_{out}) zones, a minimum temperature (T_{equiv}) after the condensation step to prevent ice formation in the HVAC system, and by ensuring conservation of energy around the crop ($I_{net} - LH - SH = 0$). Further, a maximum fogging flow ($\dot{m}_{w,fog,max}$) and LED waste heat absorption by the water cooling ($f_{LED\ cooling}$) should not be exceeded. At the night or dark period, the total (as opposed to specific) energy consumption was minimised (with different temperature setpoints) as the high sensitivity of yield to lighting and temperature was assumed only for the photoperiod. Mathematically the optimisation can be expressed as:

$$\text{Minimise} \quad \begin{matrix} E_{total} & \text{if } I_{net} = 0 \\ SE_{hourly} & \text{if } I_{net} > 0 \end{matrix}$$

By setting hourly values for

$$\begin{array}{ll} F_{hvac}, T_{hvac,out}, RH_{hvac,out}, f_{a2a,share}, u_{air,a2a,ext} & \text{for PF} \\ F_{hvac}, T_{hvac,out}, RH_{hvac,out}, F_{air,a2a,ext}, u_{air,a2a,ext}, m_{w,fog} & \text{for CGH} \\ F_{hvac}, T_{hvac,out}, RH_{hvac,out}, F_{air,a2a,ext}, u_{air,a2a,ext}, m_{w,fog}, F_{vent} & \text{for OGH} \end{array}$$

$$\begin{array}{ll} \text{Subject to} & AER_{vent} + AER_{hvac} > AER_{min} \\ & VPD_{min} < VPD_{in}, VPD_{out} < VPD_{max} \\ & T_{min} < T_{in}, T_{out} < T_{max} \\ & m_{w,fog} < \dot{m}_{w,fog,max} * A_{growing} \end{array}$$

for GHs

$$0 < f_{LED\ cooling} < 0.85$$

$$I_{net} - LH - SH = 0$$

$$T_{equiv} > 3$$

A description of the terms can be found in the nomenclature (SI) and details of how the optimisation was carried in a computational algorithm can be found in SI 6.

2.4 Scenario and sensitivity analysis

There is a host of parameters that will influence the outcome of the optimisation. Some of these are assumptions related to physical behaviour which may vary within a certain range, and others can be directly influenced by the grower, either through facility design or the level of climate control automation. For practical relevance, a comprehensive range of scenarios or settings of these parameters is assessed for a winter month (short daytime) and a summer month (long daytime) in Stockholm, further described in SI 7 and shown in Figure 5 and 6 in the results section. The standard settings are as described in the previous sections and as listed in the parameter table (table 1); the assessed crop is the vegetable basket proxy. Further assumptions adopted in this work, as well as some limitations, are listed in SI 8.

3. Results and discussion

First, the functionality of the model and the climate control operations in the three CEA systems are visualised on an hourly basis. Figure 3 shows the optimised hourly climate profiles and the specific energy consumption, while Figure 4 shows the water and CO₂ loss of the three systems for a winter month and a summer month, respectively, in Stockholm. The location and the months have been chosen to demonstrate how the climate control regulates the conditions in the OGH differently. The hourly external climate conditions are shown in Figure S9 (SI).

Second, the results of the scenario analysis are presented to assess the parametric sensitivity of the model by way of the difference to the base case for space conditioning energy (i.e. climate control) and specific energy consumption. Figure 5 shows the results for winter and Figure 6 for summer

conditions. The difference in resource consumption (water and CO₂) for each scenario is shown in SI 9 for winter (Figure S10) and summer (Figure S11).

Third, the optimisation results for the different locations are shown, broken down into the contributions by equipment to the specific energy consumption and the water and CO₂ loss.

3.1 Hourly optimisation and seasonal behaviour

Figure 3 reveals how the climate control affects inside climate conditions and Figure 4 how it affects the energy and resource consumption. For GHs in winter, night-time heating is alternated with low space conditioning requirements during the day, while ventilation was not chosen by the optimisation in the OGH to achieve high CO₂ levels and reduce heating requirements. The higher CO₂ levels from the start in the CGH result in a slightly higher yield and more favourable specific energy consumption but also higher CO₂ loss from infiltration (green dotted line). The PF in turn benefits from colder outside temperature during the night-time photoperiod, resulting in increased air-to-air cooling and refrigeration cycle efficiency. This benefit is lost in July as temperatures are higher than in winter. However, the year-round electricity consumption of LEDs was in great excess compared to the low energy consumption for air conditioning. The warmer summer puts the OGH at a considerable advantage over the CGH, in which ventilation, paired with fogging at the highest daytime temperatures, was chosen by the optimisation to regulate the climate. However, this comes at the cost of considerable water loss. In summer, the yield in the CGH is higher than in the PF due to the slightly higher radiation despite light seasonal whitewash, which was chosen by the optimisation to reduce cooling requirements. Despite the slightly lower yield in the OGH due to near-ambient CO₂ levels, specific energy consumption is lower compared with the CGH, which only relies on mechanical dehumidification and cooling. It is worth noting that in the modelling for regions with hot summers in which the outside temperature is higher than the permissible maximum temperature, venting was not an option, and the OGH behaved like the CGH, with dehumidification and fogging used to control the climate.

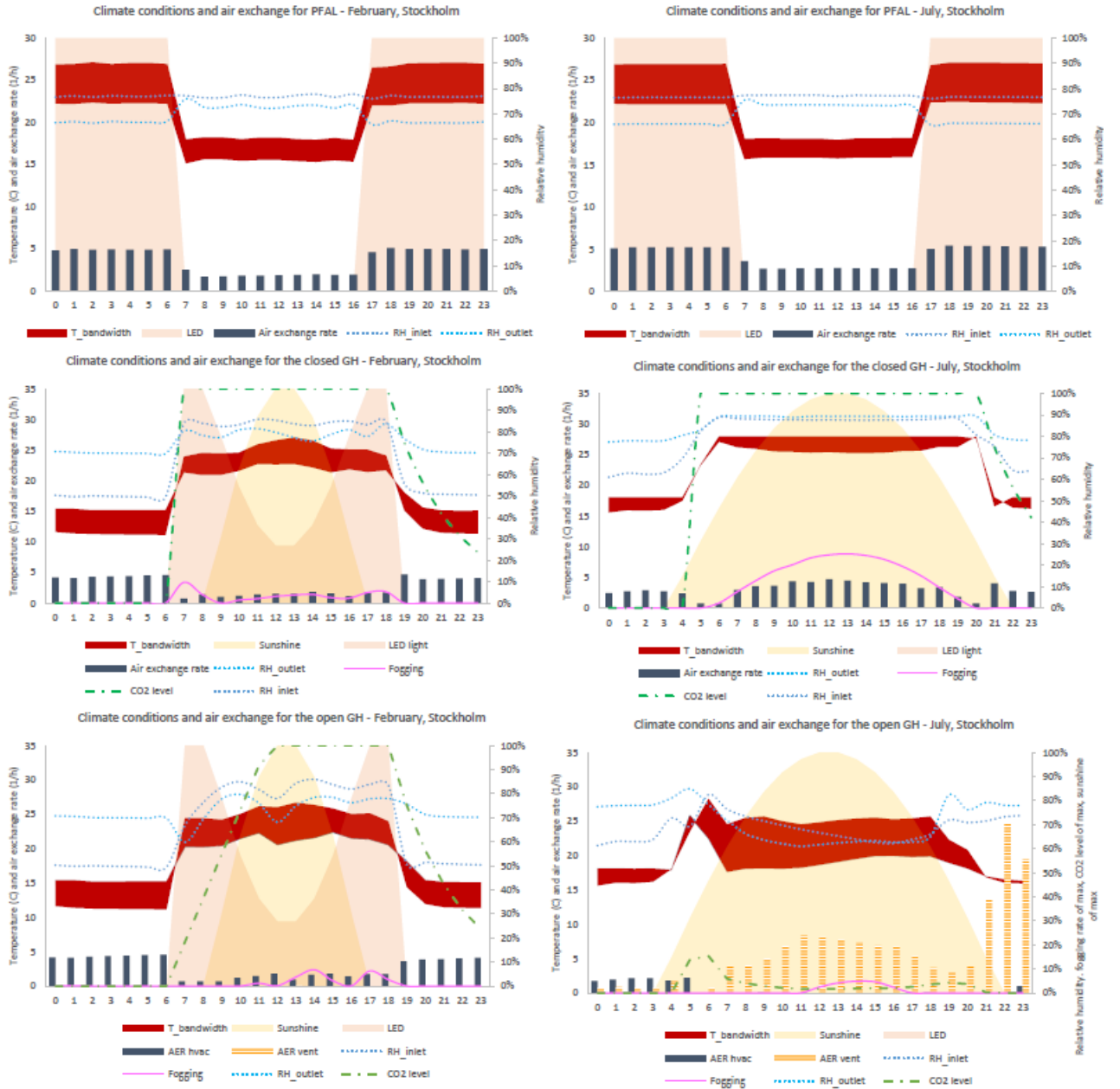


Figure 3: Optimised hourly climate control profile of the three CEA systems for a typical day in February (winter, left) and July (summer, right). The temperature is shown as a bandwidth between inlet and outlet zone, the air exchange rate displayed as a bar is in volumes/h (first y-axis), the solar radiation, LED intensity, relative humidity (inlet and outlet zone), CO2 level and fogging are displayed as percentage of their maximum (second y-axis).

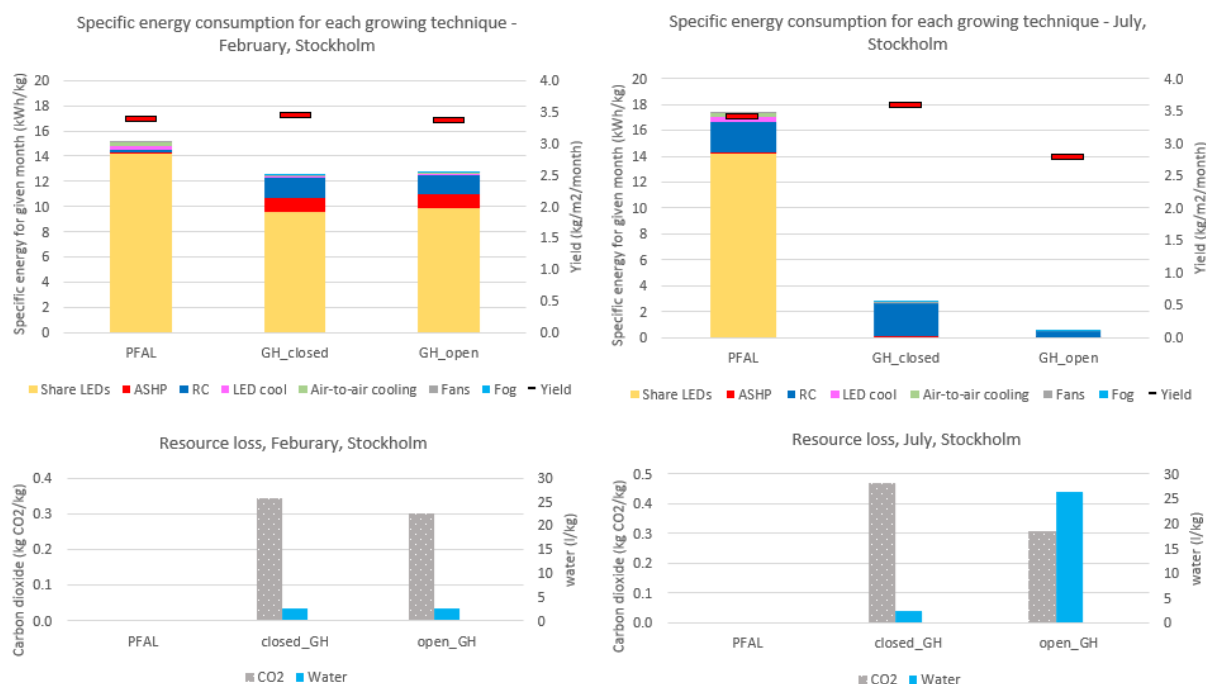


Figure 4: Specific energy consumption and resource intensity of the three CEA systems for a typical day in February (winter, left) and July (summer, right). All values are given per kg of edible produce and the obtained yield for the respective month is indicated in the second y-axis. Fan electricity consumption is displayed for HVAC duct and venting fans (Fans) and the process and air side fans of the (re)heating system (ASHP) and cooling cycle (RC). Plant uptake of water and CO₂ was equal and comparatively small and is thus excluded in this comparison.

3.2 Influence of physical, design and control variables

The variables describing the physical behaviour of plants and equipment show some sensitivity affecting the comparative results between the CEA system (Figures 5 & 6):

- The sensitivity of specific energy consumption to stomatal resistance (scenario 1) is generally very little and was highest when it would affect the venting performance in the OGH.
- A narrower VPD range (scenario 2), which some crops and growers might prefer, would greatly reduce the benefit of open venting compared to closed GHs.
- Increased LED efficiency (scenario 3) is more beneficial to plant factories than to open or closed GHs.
- A higher U-value (scenario 4, e.g. from cheaper cover material), significantly increases climate control energy consumption for GHs but slightly reduces it for PFs (similar to

Graamans et al. [33]). Due to increased heat loss, cool morning air in the Scandinavian summer could not be used for ventilation in the OGHs anymore without violating the permissible minimum temperature (thus reducing the ventilation benefits in OGHs). The lower U-value helps with daytime cooling in the CGH.

- All systems benefited slightly from a lower (heat exchange) temperature difference in the condenser and evaporator of the refrigeration cycle (scenario 5); however, this would require more heat exchange area than specified in the assumed design, when operating at the highest loads.

Scenarios 6 to 14 describe facility design and operation choices that the grower can influence:

- If the growing space is smaller (while keeping the dimensions of the HVAC system unchanged, scenario 6), the cooling efficiency becomes higher in summer for CGH and PF and also in winter for PF.
- Incorporating a square geometry (scenario 7) reduces the temperature and humidity gradient slightly and thus favours summer venting in the OGH.
- Halving the size of the heat exchangers (scenario 8) increases velocity and pressure drop at the same duty, hence leads to reduced air conditioning efficiencies, especially for cooling as the air-to-air cooling duty is reduced as well. The appropriate sizing of the HVAC units is thus of paramount importance.
- Aiming to boost production by doubling the DLI received by the plants (scenario 9) increases the specific energy consumption in the CGH and PF as the yield increase is less than the increases in the electricity consumption for LEDs and their cooling. In some cases, this might still lead to higher profits; hence this trade-off needs to be carefully considered. The OGH differs as the increased cooling load in summer can be realised through ventilation.
- The OGH also benefits in summer from an unconstrained CO₂ supply (scenario 10) but this comes at high resource costs (increase from 0.3 to 10.1 kg CO₂/kg crop, see SI S11). The influence on specific energy consumption of the preferred temperature of grown crops

(scenarios 12 and 13) is significant and the results are somewhat counterintuitive. A colder climate preference leads in all cases to greatly increased cooling and dehumidification requirements, in particular in the OGH when venting alone was no longer sufficient, suggesting that some cold temperature crops might best be grown outside in some locations. It needs to be noted, however, that the specific energy consumption of the OGH is ~7 times less than that of the CGH in the base scenario to which those percentage values refer. Studies comparing GHs and PFs could unintentionally favour one system over the other by using disadvantageous colder climate setpoints in GHs (e.g. Graamans et al. [14]). If plants prefer warmer temperatures, electricity consumption goes up in winter for all three systems but the response differs in summer; the CGH benefits from reduced daily average cooling requirements while the OGH needed to resort to mechanical dehumidification in the early evening (contrary to the purely positive response to higher temperatures from Golzar et al. [49]). This means that despite achieving artificial climate conditions in GHs, the choice of crop should still be tailored to the local climate for maximum resource efficiency [12]. Switching to mild temperature cultivars or climate setpoints in PFs in winter could reduce electricity consumption for the HVAC by over 50%. The lettuce crop (scenario 11) is closest to the cold climate preference but has a significantly higher yield than the vegetable basket proxy. Small increases in air conditioning requirements were counterbalanced by higher yields in winter, while this yield increase was not sufficient in GHs in summer to balance the much higher air conditioning requirements.

Change in climate control and specific energy consumption for 19 scenarios compared with the base scenario, February (winter) in Stockholm

System	Scenario number / Scenario name																		
	1	2	3	4	5	6	7	8	9	10	11	12	13	14	15	16	17	18	19
CGH	Difference climate control vs. base																		
	-5.9%	27.1%	-3.3%	93.0%	-4.8%	-6.3%	-0.8%	15.8%	34.4%		4.1%	58.3%	13.4%	2.1%	0.2%	-2.4%	12.0%	6.0%	119.9%
OGH	Difference specific energy vs. base																		
	-0.8%	7.5%	-16.7%	23.2%	-1.0%	-1.6%	0.2%	5.4%	37.2%		-40.0%	15.7%	2.4%	1.3%	0.8%	6.9%	5.1%	1.4%	116.4%
OGH	Difference climate control vs. base																		
	-6.9%	27.3%	1.6%	104.7%	-2.6%	-5.8%	2.0%	17.9%	35.4%	0.2%	3.8%	35.4%	17.1%	0.0%	4.6%	-0.7%	10.4%	9.5%	34.6%
OGH	Difference specific energy vs. base																		
	-1.3%	7.2%	-15.9%	24.7%	-0.9%	-1.8%	0.2%	5.2%	34.9%	-2.2%	-41.2%	10.2%	3.2%	0.0%	1.2%	4.6%	5.5%	2.1%	6.4%
PFAL	Difference climate control vs. base																		
	18.8%	38.2%	-26.2%	-10.0%	-1.9%	-37.1%	6.7%	90.2%	252.5%		-18.0%	63.6%	57.4%	349.9%		-8.6%	-1.3%	93.9%	309.1%
PFAL	Difference specific energy vs. base																		
	0.1%	-0.1%	-21.4%	-1.0%	-0.3%	-4.4%	0.0%	6.3%	19.3%		-39.4%	6.2%	1.0%	21.0%	-0.9%	0.0%	4.9%		56.4%
	rmin 82	VPD 0.6-1 kPa	75% LED eff.	Double U-value	lower dT RC	Half size	Square geometry	Half HEX area	Double DLI	No CO2 limit	Lettuce	Cold climate ..	Warm climate ..	No LED water..	LED fixed intensity	Energy mi nimisati..	no air-to-air..	LED cooling on	Yield maxi misation

Figure 5: Percentage change of climate control and specific energy consumption for the three CEA system and 19 scenarios compared with the base scenario for February (winter) in Stockholm

The remaining scenarios considered cases with less sophisticated climate control capacities:

- Opting to not have water-cooled LEDs (scenario 14) had significant negative consequences in the PF, however, for GHs the cost of such systems needs to be weighed against modest improvements in specific energy consumption.
- Scenario 15 investigated the effect of employing fixed-intensity LEDs. In the PF, this led to longer but less intense photoperiods (18 instead of 15 hours) which showed to be beneficial for climate control. However, some plants might require longer dark periods for healthy growth. Contrary to initial expectations, the constant supply of light and heat in GHs in winter had only a small effect on specific energy consumption. Growers need to evaluate the trade-off between higher control complexity and small total energy savings.
- If a control system aims to merely consider minimised energy consumption (scenario 16), the specific energy consumption would increase due to lower yields. Although this effect was

1 relatively small, higher productivity has the most impact on profit which would justify a
2 combined yield-energy approach.

- 3 • Scenario 17 describes facilities that do not employ air-to-air cooling. In winter, this led to a
4 considerable increase in energy consumption, in particular for the PF which benefits from
5 colder night-time temperatures during the photoperiod. The effect in summer was negligible.
6 The other cooling device, the fogging system, was of paramount importance. Cooling through
7 “ventilation and mechanical cooling only” lead to dramatic increases in specific energy (data
8 not shown) for March in Singapore (+279% and +158%% for the CGH and OGH, respectively)
9 and considerable increases for July in Stockholm (49% and 0.4% for the CGH and OGH,
10 respectively).
- 11 • LED cooling might be detrimental for GHs if it is always on and takes away otherwise useful
12 heat, as shown by scenario 18 (the base scenario considers flexible cooling).
- 13 • Optimising solely for hourly yield resulted in very high energy consumption for climate
14 control in all cases. The increase in specific energy was particularly significant for
15 greenhouses in summer (6.6 and 18.2 times as much for the CGH and OGH), when intensive
16 mechanical cooling was used to closely control the climate, rather than venting. The increase
17 in yield, however, was comparably insignificant in PFs (2-2.4%) and small for GHs in summer
18 (10.8% for the CGH and 38.9% for the OGH), not enough to justify controlling the facility in
19 this way.

20 The sensitivity of the scenarios on water and CO₂ loss through venting and infiltration is small (Figure
21 S10 and S11); the biggest effect on water loss is observed for increasing the DLI and for lettuce
22 (scenario 9 and 11, specific consumption drops as yield increases), for warm climate preferences
23 (scenario 13, increased loss due to higher water vapour storage capacity of air), in the OGH due to
24 increased venting for no air-to-air cooling during winter (scenario 17), in summer for cold climates
25 (scenario 12) and in summer when maximising the yield (scenario 19). The response to the
26 parameters can be divided into positive or negative proportional (scenarios 3,5,6,8,10,12,14,16,18)

and non-proportional or non-linear (scenarios 1,2,4,7,9,11,13,15,17,19), with the latter responses fully depending on the CEA system and the outside climate. This means that results obtained in the study may be proportionally adjusted to other cases only for the proportional parameters.

Change in climate control and specific energy consumption for 19 scenarios compared with the base scenario, July (summer) in Stockholm

		Scenario number / Scenario name																		
System		1	2	3	4	5	6	7	8	9	10	11	12	13	14	15	16	17	19	
CGH	Difference climate control vs. base	-4.9%	21.2%		-19.4%	-10.3%	-37.1%	-1.4%	96.0%	187.6%			55.0%	119.3%	-41.8%		0.1%	7.3%	743.3%	
	Difference specific energy vs. base	-4.6%	21.0%		-19.6%	-10.4%	-37.3%	-1.5%	95.1%	62.6%		10.2%	111.7%	-42.3%			0.0%	7.5%	662.7%	
OGH	Difference climate control vs. base	-25.5%	191.1%		80.4%	-11.4%	-7.4%	-10.8%	5.3%	-4.5%	-6.9%	171.2%	351.0%	27.2%			0.0%	0.9%	2746.1%	
	Difference specific energy vs. base	-25.4%	175.0%		72.1%	-10.9%	-7.5%	-10.7%	5.5%	-44.5%	-33.3%	90.5%	363.8%	21.3%			0.0%	0.9%	1820.6%	
PFAL	Difference climate control vs. base	3.8%	23.1%	-14.3%	-1.8%	-7.1%	-20.2%	1.4%	38.0%	120.3%		1.5%	38.5%	-2.1%	141.9%	-4.5%	-0.9%	16.5%	349.3%	
	Difference specific energy vs. base	-0.7%	2.0%	-19.0%	-0.2%	0.4%	-2.7%	-0.4%	6.8%	15.4%		-35.3%	9.5%	-3.2%	23.4%	-21.9%	0.6%	2.0%	59.2%	
		rmin 82	VPD 0.6-1 kPa	75% LED eff.	Double U-value	lower dT RC	Half size	Square geometry	Half HEX area	Double DLI	No CO2 limit	Lettuce	Cold climate ..	Warm climate ..	No LED water ..	LED fixed intensity	Energy minimis ..	no air-to-air ..	Yield maximisation	

Figure 6: Percentage change of climate control and specific energy consumption for the three CEA system and 19 scenarios compared with the base scenario for July (summer) in Stockholm

3.3 Location-dependent comparative performance

Figure 7 shows great differences between the three systems and between the locations, in particular for the OGH. The PF has increased specific energy consumption in hot regions where mechanical cooling is more challenging and higher specific energy requirements in all locations. Interestingly, despite a higher average temperature in UAE compared with Singapore, a lower night-time temperature during peak cooling demand led to lower specific energy consumption in PFs in UAE. The effect of seasonal temperature extremes becomes apparent in the GHs; while Tokyo's average annual solar radiation is lower than in Tasmania or Santiago (listed from lowest to highest solar radiation in Figure 7), it does not require additional lighting. On the other hand, constantly high temperatures are detrimental for Singapore and Maricopa in a GH without venting but with the

Specific energy consumption of each system in ten different locations

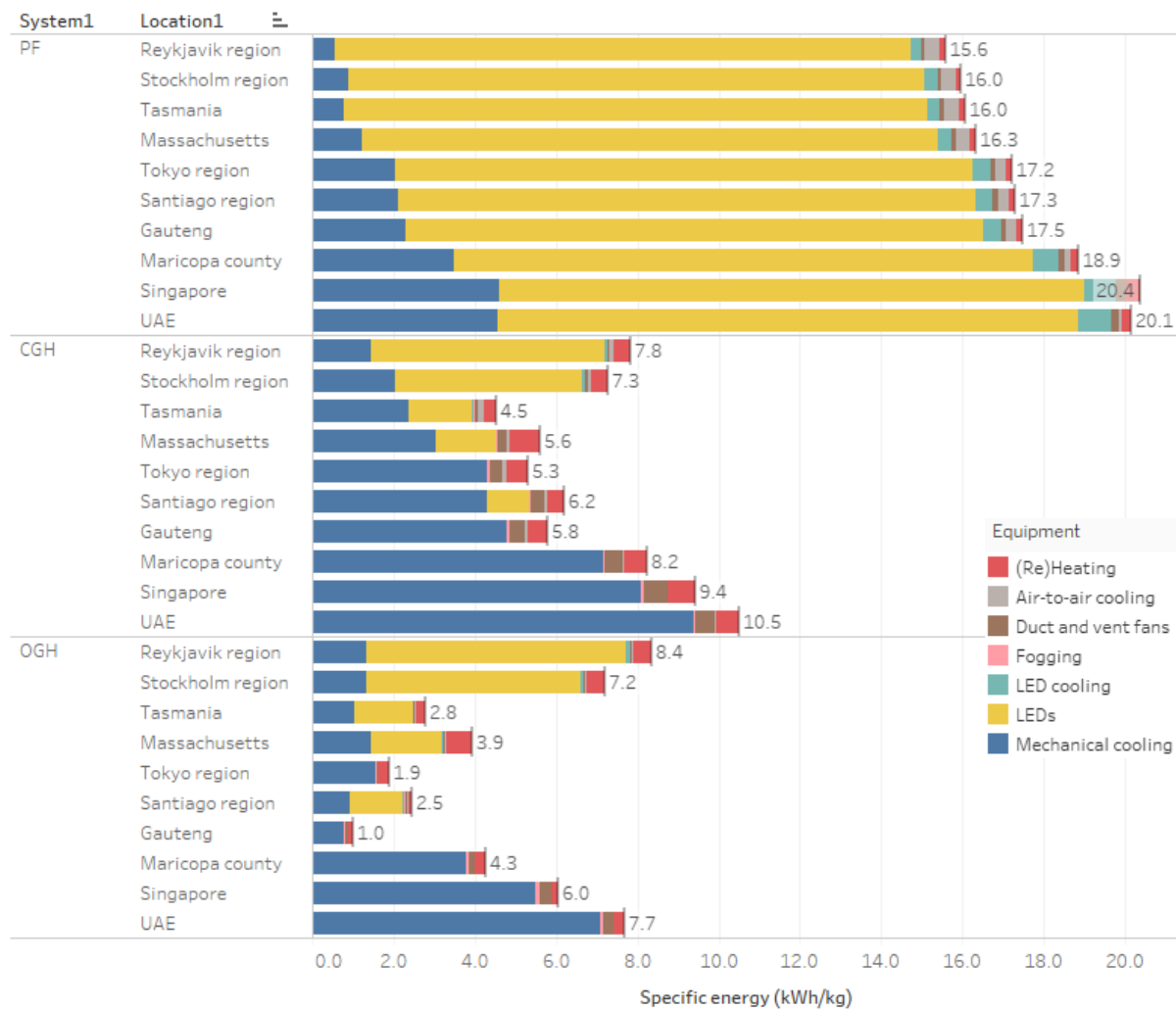


Figure 7: Average annual specific energy consumption of the three systems (PF, CGH, OGH) at different locations. The locations are sorted by their average annual temperature in ascending order. Process side fan electricity consumption was allocated to (re)heating and mechanical cooling.

- 1 option to vent, the specific energy can be lower than in the colder regions of Stockholm and
- 2 Reykjavik. In UAE, temperatures are too high for venting most of the time, leading to only a slight
- 3 reduction in specific energy consumption for the OGH. In very cold regions such as around Reykjavik,
- 4 ventilation was not chosen by the optimisation as it would significantly increase heating
- 5 requirements, which means OGH and CGH have similar results. The reason for the higher specific
- 6 energy in OGHs in Reykjavik is due to a restriction of hourly CO₂ supply in OGHs imposed in the
- 7 model to avoid unacceptable CO₂ loss in ventilation, which lead to lower yields in the morning hours
- 8 (see green dashed line Figure 3). In general, the reduction of specific energy in OGHs compared with

CGHs is highest when ventilation could be used as a major contributor to climate control. Figure S12 (SI) shows the water and CO₂ loss incurred from the exchange with the environment in GHs for all locations. The CO₂ loss per kg crops is relatively constant with ~0.35 kg for the CGH and ~0.31 kg for the OGH. Venting in the OGH significantly increases water loss and represents thus a trade-off with energy consumption in water-scarce regions. The hourly load curves for each month and location are displayed in figure S13.

None of the locations had sufficient solar radiation to justify installing a refraction lens cover as described by Pakari and Ghani [50]. This was due to a lower target DLI considered optimum for plant growth in their work (8.1 mol/m²/day compared with 13.7 mol/m²/day in the current study). A calculation of the effect of the cover for the hottest months in UAE by adjusting the yield akin to scenario 9 resulted in a reduction of both cooling requirement and specific energy consumption of around 40% for both GHs. If the solar transmission of the lenses can be increased (e.g. by reducing the spacing between them), it constitutes an attractive option for energy-efficient high-yield GH production in the desert.

3.4 Comparison with other studies

Comparison of the results from this work and those from previous studies is far from straightforward due to differences in both the adopted problem settings (e.g. temperature preference, DLI requirements and growing intensities of individual crops) and the slightly different choice of locations. Nevertheless, an attempt has been made to make the results of several relevant studies as comparable as possible; the details of the needed conversions and adjustments can be found in SI 10. Here, key contrasts to the specific energy consumption of GHs and PFs are presented in Figure 8 – which needs to be interpreted with caution due to the aforementioned discrepancies between different studies. Those differences that can be sensibly linked to the variation in the modelling approaches are discussed below.

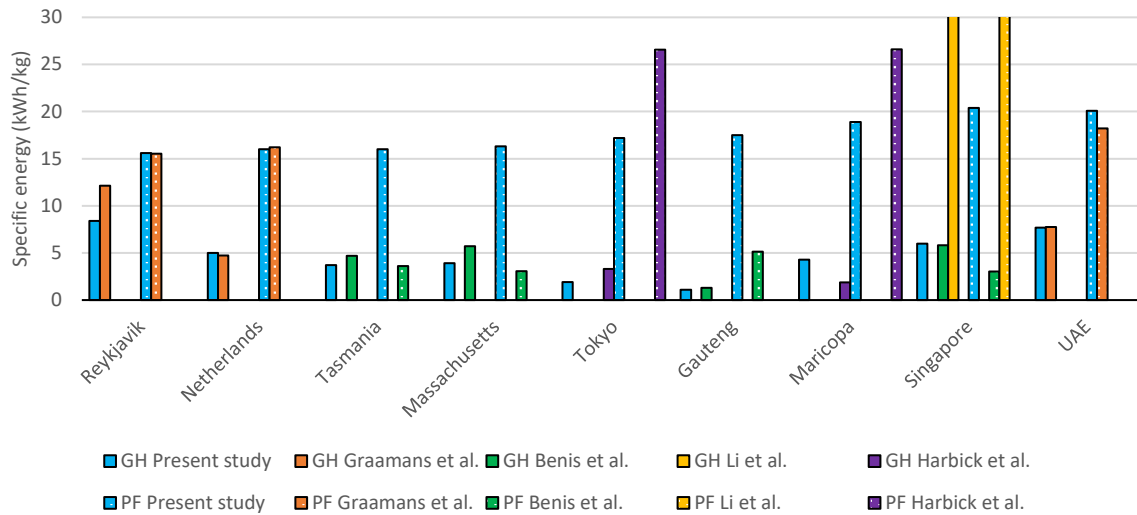


Figure 8: Specific energy comparison of this work with previous studies, adjusted for yield according to light levels (see SI 10). The adjusted specific energy for Li et al. is 113.9 kWh/kg for GHs and 59.1 kWh/kg for PFs.

Comparing the results from this study with those from Li et al. [13] who conducted an optimisation for glass-covered (similar to OGH) and opaque (similar to PF) shipping containers for Singapore, it was found that cooling electricity requirements were significantly different. Cooling was a magnitude more energy-intensive in GHs (explained by their equal electricity consumption and cooling needs in kW terms implying a COP of 1, compared with an average COP of around 6.5 for Singapore in this work) and multiple times more for PFs in their work (due to a higher U-value of the walls).

Benis et al. [14] reported a similar water consumption per kg produce and a slightly higher specific energy consumption for the OGH. The difference can partly be explained by the optimised interplay of mechanical cooling, fogging and ventilation in the present study. The opaque shipping containers had a similar share between the energy consumption for cooling and lighting. However, their specific energy consumption was significantly lower compared with the present study. This can be explained by the reported ~ 3.2 kWh lighting per kg crops (or 47 W/m^2 for 13 hours), which is significantly below what the current study considers necessary to achieve the reported yield with current LED technology.

1 An indicative comparison with Graamans et al. [14] showed similar energy intensities except in a few
2 cases. In the cold climate, the lower specific energy consumption is due to the modelling of
3 consistent production using supplemental lighting during winter months in this work, making them
4 more favourable in such climates. In UAE, this work had a higher specific energy consumption, mainly
5 due to higher energy use for climate control, which likely stems from the fixed COP assumed in their
6 study compared with a detailed variable model for the COP in this work. Their work did not report
7 data for locations which particularly benefitted from a more sophisticated GH climate control, where
8 it would be possible to greatly reduce energy demand for OGHs.

9 The difference for the PF in Harbick and Albright [23] is primarily due to their high heating
10 requirements from a poorly insulated building, with lower light efficacy playing a minor role. The
11 lower specific energy consumption in Phoenix for the GH in their work is due to their model relying
12 on evaporative cooling, which would have caused excessive moisture levels in this work. The higher
13 specific energy consumption in the milder location is likely due to sub-optimal climate control.

14 *3.5 Recommendations for practitioners*

15 From the parametric sensitivity analysis reported in section 3.2, recommendations can be derived to
16 reduce the energy required for growing. CEA systems benefit from tailoring crops and cultivars to the
17 ideal climate conditions (e.g. tolerating higher temperatures) and adequate sizing of the HVAC
18 system. GHs benefit from covers with low U-values and advanced control systems which can regulate
19 ventilation, fogging and mechanical cooling according to outside conditions. In water-stressed
20 regions, the degree of ventilation can be assessed on a temporal basis (e.g. the extent of seasonal
21 rainfall). Fully closed GHs make sense only if the pest risk is constantly high and significant
22 productivity increases can be realised through high CO₂ levels. There is less justification from an
23 energy perspective for greenhouse operators to invest in LED water cooling (unless symbiotic effects
24 with a host building can be realised), air-to-air cooling in combination with electricity-driven heating
25 and cooling (as process side heat recovery is preferred) and complicated LED dimming schedules.

1 However, those technologies, together with efficient LEDs, are highly recommended for PFs. Indoor
2 growers need to be aware that maximising yield may come at higher specific energy requirements
3 and thus environmental footprints.

4 The choice of CEA system and design in a given location depends on many factors. The source of
5 electricity (i.e. fossil vs renewable) combined with the specific energy consumption will dramatically
6 influence the carbon footprint of the produce. Although the specific energy consumption is a main
7 aspect for the sustainability of controlled-environment vegetable production, other factors, such as
8 profitability or land availability, might be more important for growers. Thus, if land is scarce and
9 expensive, PFs might still be favourable as growing layers and rooms can be stacked as desired.
10 Additionally, existing (urban) space such as empty parking lots and abandoned buildings reduce the
11 upfront cost and environmental impact from the structure. Nevertheless, rooftop and peri-urban
12 GHs, compared to other CEA options, present the most favourable alternative to open-field farming
13 in most cases.

14 **4. Conclusions**

15 This work investigates and compares the best-practice energy intensity of CEA systems (plant
16 factories and open and closed greenhouses) for several climate zones. A novel optimisation approach
17 was developed that combines a detailed modelling of electrified climate control systems in relation
18 to the outside climate conditions (temperature, humidity, solar radiation) with spatially and
19 temporally varying vegetable yields dependent on the interior climate conditions realised in these
20 systems. It provides a consistent and improved basis for comparison between not just the three CEA
21 systems but also different climate conditions and technical or operational choices and their effect on
22 specific energy and resource consumption.

23 The approach has been used for hourly optimisation of CEA systems for a whole year in ten different
24 human habitat locations representing a diverse range of climatic conditions. The results indicate that
25 plant factories (i.e. vertical indoor farming systems) are more energy-intensive than greenhouses in

all climates. The specific energy consumption of ventilated OGHs is significantly lower than the other two systems, even in more extreme climate, although at a higher level of water consumption. While the lower energy intensity of OGHs is not always contrary to previous studies, the extent of the difference between OGHs and other options identified in this work is stronger than generally reported. This increased favourability of GHs, and especially OGHs, in this work is mainly due to the possibility of optimising greenhouse control.

In addition to the assessment of different locations using the representative parameter settings, the optimisation approach has also been applied to one location for a comprehensive range of parametric sensitivities to understand the impact of assumptions and technical and operational variations. These changes do not significantly change the overall favourability of OGHs but do offer some recommendations for practitioners. The most relevant ones for energy-efficiency are harmonising crop choice (and their preferred temperature range) with local climate conditions in GHs, considering operating at modest DLI levels and installing LED water cooling in PFs.

A range of open research questions for energy-efficient CEA remains. From a plant science perspective, the breeding of high-yield cultivars thriving in controlled environments is yet in its infancy, and an open-access compendium relating yield values of multiple crops and cultivars to light intensity (and respective climate conditions during experiments) would bring substantial benefits to the CEA community. From an energy perspective, the quantitative benefits of geothermal and waste heat for GHs (for direct heating but also enabling vapour absorption refrigeration), the influence of seasonal and daily solar heat storage and transparent PV panels in GHs, and industrial and building symbiosis for GHs and PFs require further assessment. From a life-cycle-assessment perspective, the trade-off between building PFs in existing structures close to the consumer and GHs with higher transport (crop and workers) requirements need to be assessed, in particular in locations where the difference in specific energy consumption was less pronounced. Future studies should consider the influence of climate setpoints and crop selections when comparing PF and GH in different locations, and consider choosing different crops for different seasons in modelling studies.

Finally, it is important to note that obtaining the performance indicated in this study requires advanced climate control devices which might not always be available to growers. The modelling methodology employed in this study may be used to determine the optimum (hourly) set points for energy-efficient operations, while the actual sensing and actuator control needs to be programmed via control loop mechanisms (not addressed in this work). Results derived in this work for the vegetable basket can be adapted to specific crops by figuring out the respective yield at light levels of 13.5 mol/m²/day and adjusting the specific energy consumption proportionally. The influence of different climate setpoints is akin to the changes described in section 3.2.

Author contributions:

Till Weidner has developed the methodology, conducted the analysis and wrote the original draft. Michael Hamm has conceptualised the work, validated the methodology and reviewed and edited the draft. Aidong Yang has aided in the conceptualised and development of the methodology, supervised Till Weider, validated the model and calculations and reviewed and edited the draft.

Acknowledgements:

Financial support for TW for the duration of his PhD project by the Clarendon Fund is greatly appreciated. We are grateful to Adam Bowler from Oxford Air Conditioning Ltd. for guidance for the design of the air conditioning system, to Scottie Wang from CoolingHouse for guidance on LED water cooling and to UrbanOasis in Stockholm for a tour of vertical farming operations and climate control systems, and to Tim Adams who proofread the manuscript.

Declaration of competing interest:

The authors declare that they have no known competing financial, professional or personal interests that could have appeared to influence the work reported in this paper.

Abbreviations:

ASHP Air source heat pump

CEA Controlled environment agriculture

1	CGH	Closed, non-ventilated greenhouse
2	COP	Coefficient of performance
3	ET	Evapotranspiration
4	GH	Greenhouse
5	GHI	Global horizontal irradiation
6	HEX	Heat exchanger
7	HVAC	Heating, ventilation and air conditioning system
8	LED	Light-emitting diode
9	OGH	Open, ventilated greenhouse
10	PAR	Photosynthetically active radiation
11	PF	Plant factory or indoor vertical farming facility
12	PFR	Plug flow reactor
13	PPM	Parts per million
14	RC	Refrigeration cycle
15	RLC	Refraction lens cover
16	VPD	Vapour pressure deficit

17 **References**

- 18 [1] Willett W, Rockström J, Loken B, Springmann M, Lang T, Vermeulen S, et al. Food in the
19 Anthropocene: the EAT–Lancet Commission on healthy diets from sustainable food systems.
20 Lancet 2019;393:447–92. [https://doi.org/10.1016/S0140-6736\(18\)31788-4](https://doi.org/10.1016/S0140-6736(18)31788-4).
- 21 [2] Harris J, Depenbusch L, Pal AA, Nair RM, Ramasamy S. Food system disruption: initial
22 livelihood and dietary effects of COVID-19 on vegetable producers in India. Food Secur
23 2020;12:841–51. <https://doi.org/10.1007/s12571-020-01064-5>.
- 24 [3] Béné C. Resilience of local food systems and links to food security – A review of some
25 important concepts in the context of COVID-19 and other shocks. Food Secur 2020;12:805–22.
26 <https://doi.org/10.1007/s12571-020-01076-1>.
- 27 [4] Hamm M, Frison E, Tirado von der Pahlen M. Human health, diets and nutrition: missing links
28 in eco-agri-food systems. TEEB Agric Food Sci Econ Found 2018.
- 29 [5] O’Sullivan CA, Bonnett GD, McIntyre CL, Hochman Z, Wasson AP. Strategies to improve the
30 productivity, product diversity and profitability of urban agriculture. Agric Syst 2019;174:133–
31 44. <https://doi.org/10.1016/j.agsy.2019.05.007>.
- 32 [6] Barbosa GL, Almeida Gadelha FD, Kublik N, Proctor A, Reichelm L, Weissinger E, et al.
33 Comparison of land, water, and energy requirements of lettuce grown using hydroponic vs.
34 Conventional agricultural methods. Int J Environ Res Public Health 2015;12:6879–91.
35 <https://doi.org/10.3390/ijerph120606879>.
- 36 [7] IEA. World Energy Outlook 2019. Paris: 2019.
- 37 [8] Shiina T, Hosokawa D, Roy P, Orikasa T, Nakamura N, Thammawong M. Life cycle inventory

- analysis of leafy vegetables grown in two types of plant factories. *Acta Hortic* 2011;919:115–22. <https://doi.org/10.17660/ActaHortic.2011.919.14>.
- [9] Iddio E, Wang L, Thomas Y, McMorro G, Denzer A. Energy efficient operation and modeling for greenhouses: A literature review. *Renew Sustain Energy Rev* 2020;117:109480. <https://doi.org/10.1016/j.rser.2019.109480>.
- [10] Ahemd HA, Al-Faraj AA, Abdel-Ghany AM. Shading greenhouses to improve the microclimate, energy and water saving in hot regions: A review. *Sci Hortic (Amsterdam)* 2016;201:36–45. <https://doi.org/10.1016/j.scienta.2016.01.030>.
- [11] Y. Tong, T. Kozai, N. Nishioka, K. Ohyama. Reductions in Energy Consumption and CO₂ Emissions for Greenhouses Heated with Heat Pumps. *Appl Eng Agric* 2012;28:401–6. <https://doi.org/10.13031/2013.41488>.
- [12] Li L, Li X, Chong C, Wang CH, Wang X. A decision support framework for the design and operation of sustainable urban farming systems. *J Clean Prod* 2020;268:121928. <https://doi.org/10.1016/j.jclepro.2020.121928>.
- [13] Graamans L, Baeza E, van den Dobbelsteen A, Tsafaras I, Stanghellini C. Plant factories versus greenhouses: Comparison of resource use efficiency. *Agric Syst* 2018;160:31–43. <https://doi.org/10.1016/j.agry.2017.11.003>.
- [14] Benis K, Reinhart C, Ferrão P. Building-Integrated Agriculture (BIA) In Urban Contexts : Testing A Simulation-Based Decision Support Workflow. 15th IBPSA Conf. San, 2017.
- [15] Weidner T, Yang A. The potential of urban agriculture in combination with organic waste valorization: Assessment of resource flows and emissions for two european cities. *J Clean Prod* 2019;244:118490. <https://doi.org/10.1016/j.jclepro.2019.118490>.
- [16] Choab N, Allouhi A, El Maakoul A, Kousksou T, Saadeddine S, Jamil A. Review on greenhouse microclimate and application: Design parameters, thermal modeling and simulation, climate controlling technologies. *Sol Energy* 2019;191:109–37. <https://doi.org/10.1016/j.solener.2019.08.042>.
- [17] Van Beveren PJM, Bontsema J, Van Straten G, Van Henten EJ. Minimal heating and cooling in a modern rose greenhouse. *Appl Energy* 2015;137:97–109. <https://doi.org/10.1016/j.apenergy.2014.09.083>.
- [18] Villarreal-Guerrero F, Kacira M, Fitz-Rodríguez E, Linker R, Kubota C, Giacomelli GA, et al. Simulated performance of a greenhouse cooling control strategy with natural ventilation and fog cooling. *Biosyst Eng* 2012;111:217–28. <https://doi.org/10.1016/j.biosystemseng.2011.11.015>.
- [19] Vanthoor BHE, Gázquez JC, Magán JJ, Ruijs MNA, Baeza E, Stanghellini C, et al. A methodology for model-based greenhouse design: Part 4, economic evaluation of different greenhouse designs: A Spanish case. *Biosyst Eng* 2012;111:336–49. <https://doi.org/10.1016/j.biosystemseng.2011.12.008>.
- [20] Golzar F, Heeren N, Hellweg S, Roshandel R. A novel integrated framework to evaluate greenhouse energy demand and crop yield production. *Renew Sustain Energy Rev* 2018;96:487–501. <https://doi.org/10.1016/j.rser.2018.06.046>.
- [21] Benis K, Reinhart C, Ferrão P. Development of a simulation-based decision support workflow for the implementation of Building-Integrated Agriculture (BIA) in urban contexts. *J Clean Prod* 2017;147:589–602. <https://doi.org/10.1016/j.jclepro.2017.01.130>.
- [22] Graamans L, van den Dobbelsteen A, Meinen E, Stanghellini C. Plant factories; crop

- 1 transpiration and energy balance. *Agric Syst* 2017;153:138–47.
2 <https://doi.org/10.1016/j.agsy.2017.01.003>.
- 3 [23] Harbick K, Albright LD. Comparison of energy consumption: Greenhouses and plant factories.
4 *Acta Hortic* 2016;1134:285–92. <https://doi.org/10.17660/ActaHortic.2016.1134.38>.
- 5 [24] Kozai T, Niu G, Takagaki M. *Plant Factory - An Indoor Vertical Farming System for Efficient*
6 *Quality Food Production*. Academic Press; 2019.
- 7 [25] Hemming S, De Zwart F, Elings A, Righini I, Petropoulou A. Remote control of greenhouse
8 vegetable production with artificial intelligence—greenhouse climate, irrigation, and crop
9 production. *Sensors (Switzerland)* 2019;19. <https://doi.org/10.3390/s19081807>.
- 10 [26] Stacey NT, Hildebrandt D. Quantitative modeling of a greenhouse as a bioreactor to process
11 power station emissions. *Environ Prog Sustain Energy* 2018;37:1774–80.
12 <https://doi.org/10.1002/ep.12824>.
- 13 [27] Zhang S, Schulman B. A Numerical Model for Simulating the Indoor Climate inside the
14 Growing Chambers of Vertical Farms with Case Studies. *Int J Environ Sci Dev* 2017;8:728–35.
15 <https://doi.org/10.18178/ijesd.2017.8.10.1047>.
- 16 [28] Kittas C, Boulard T, Papadakis G. Natural ventilation of a greenhouse with ridge and side
17 openings: Sensitivity to temperature and wind effects. *Trans Am Soc Agric Eng* 1997;40:415–
18 25. <https://doi.org/10.13031/2013.21268>.
- 19 [29] López A, Valera DL, Molina-Aiz FD, Peña A. Sonic anemometry to evaluate airflow
20 characteristics and temperature distribution in empty Mediterranean greenhouses equipped
21 with pad-fan and fog systems. *Biosyst Eng* 2012;113:334–50.
22 <https://doi.org/10.1016/j.biosystemseng.2012.09.006>.
- 23 [30] Teitel M, Ziskind G, Liran O, Dubovsky V, Letan R. Effect of wind direction on greenhouse
24 ventilation rate, airflow patterns and temperature distributions. *Biosyst Eng* 2008;101:351–
25 69. <https://doi.org/10.1016/j.biosystemseng.2008.09.004>.
- 26 [31] Arbel A, Yekutieli O, Barak M. Performance of a fog system for cooling greenhouses. *J Agric*
27 *Eng Res* 1999;72:129–36. <https://doi.org/10.1006/jaer.1998.0351>.
- 28 [32] Ghoulem M, El Moueddeb K, Nehdi E, Boukhanouf R, Kaiser Calautit J. Greenhouse design and
29 cooling technologies for sustainable food cultivation in hot climates: Review of current
30 practice and future status. *Biosyst Eng* 2019;183:121–50.
31 <https://doi.org/10.1016/j.biosystemseng.2019.04.016>.
- 32 [33] Graamans L, Tenpierik M, van den Dobbelsteen A, Stanghellini C. Plant factories: Reducing
33 energy demand at high internal heat loads through façade design. *Appl Energy*
34 2020;262:114544. <https://doi.org/10.1016/j.apenergy.2020.114544>.
- 35 [34] Russo G, Anifantis AS, Verdiani G, Mugnozza GS. Environmental analysis of geothermal heat
36 pump and LPG greenhouse heating systems. *Biosyst Eng* 2014;127:11–23.
37 <https://doi.org/10.1016/j.biosystemseng.2014.08.002>.
- 38 [35] Bakos GC, Fidanidis D, Tsagas NF. Greenhouse heating using geothermal energy. *Geothermics*
39 1999;28:759–65. [https://doi.org/10.1016/S0375-6505\(99\)00041-3](https://doi.org/10.1016/S0375-6505(99)00041-3).
- 40 [36] Nemš A, Nemš M, Świder K. Analysis of the possibilities of using a heat pump for greenhouse
41 heating in Polish climatic conditions-A case study. *Sustain* 2018;10.
42 <https://doi.org/10.3390/su10103483>.
- 43 [37] Incropera FP, DeWitt DP, Bergman TL, Lavine AS. *Fundamentals of Heat and Mass Transfer*.

- 6th ed. John Wiley & Sons; 2006.
- [38] Katsoulas N, Stanghellini C. Modelling crop transpiration in greenhouses: Different models for different applications. *Agronomy* 2019;9:1–17. <https://doi.org/10.3390/agronomy9070392>.
- [39] Stanghellini C. Transpiration of Greenhouse Crops. Wageningen University, 1987.
- [40] Villarreal-Guerrero F, Kacira M, Fitz-Rodríguez E, Kubota C, Giacomelli GA, Linker R, et al. Comparison of three evapotranspiration models for a greenhouse cooling strategy with natural ventilation and variable high pressure fogging. *Sci Hortic (Amsterdam)* 2012;134:210–21. <https://doi.org/10.1016/j.scienta.2011.10.016>.
- [41] Kuijpers WJP, van de Molengraft MJG, van Mourik S, van 't Ooster A, Hemming S, van Henten EJ. Model selection with a common structure: Tomato crop growth models. *Biosyst Eng* 2019;187:247–57. <https://doi.org/10.1016/j.biosystemseng.2019.09.010>.
- [42] Manikandan K, Vethamoni I. A review: Crop modeling in vegetable crops. ~ 1006 ~ *J Pharmacogn Phytochem* 2017;6:1006–9.
- [43] Van Henten EJ. Validation of a dynamic lettuce growth model for greenhouse climate control. *Agric Syst* 1994;45:55–72. [https://doi.org/10.1016/S0308-521X\(94\)90280-1](https://doi.org/10.1016/S0308-521X(94)90280-1).
- [44] Rijdsdijk AA, Vogelesang JVM. Temperature integration on a 24-hour base: a more efficient climate control strategy. *Acta Hortic., International Society for Horticultural Science (ISHS), Leuven, Belgium; 2000, p. 163–70.* <https://doi.org/10.17660/ActaHortic.2000.519.16>.
- [45] Shamshiri RR, Kalantari F, Ting KC, Thorp KR, Hameed IA, Weltzien C, et al. Advances in greenhouse automation and controlled environment agriculture: A transition to plant factories and urban agriculture. *Int J Agric Biol Eng* 2018;11:1–22. <https://doi.org/10.25165/j.ijabe.20181101.3210>.
- [46] Shamshiri RR, Jones JW, Thorp KR, Ahmad D, Man HC, Taheri S. Review of optimum temperature, humidity, and vapour pressure deficit for microclimate evaluation and control in greenhouse cultivation of tomato: A review. *Int Agrophysics* 2018;32:287–302. <https://doi.org/10.1515/intag-2017-0005>.
- [47] Yoder RE, Odhiambo LO, Wright WC. Effects of Vapor-Pressure Deficit and Net-Irradiance Calculation Methods on Accuracy of Standardized Penman-Monteith Equation in a Humid Climate. *J Irrig Drain Eng* 2005;131:228–37. [https://doi.org/10.1061/\(ASCE\)0733-9437\(2005\)131:3\(228\)](https://doi.org/10.1061/(ASCE)0733-9437(2005)131:3(228)).
- [48] Fick SE, Hijmans RJ. WorldClim 2: new 1-km spatial resolution climate surfaces for global land areas. *Int J Climatol* 2017;37:4302–15. <https://doi.org/10.1002/joc.5086>.
- [49] Golzar F, Heeren N, Hellweg S, Roshandel R. A comparative study on the environmental impact of greenhouses: A probabilistic approach. *Sci Total Environ* 2019;675:560–9. <https://doi.org/10.1016/j.scitotenv.2019.04.092>.
- [50] Pakari A, Ghani S. Evaluation of a novel greenhouse design for reduced cooling loads during the hot season in subtropical regions. *Sol Energy* 2019;181:234–42. <https://doi.org/10.1016/j.solener.2019.02.006>.